A Machine Learning Approach to COVID-19 Detection via Graphene Field-Effect-Transistor (GFET)

Darin Tsui[1], Francisco Downey[1], Shreenithi Navaneethan[1], Akshay Paul[1], Tyler Bodily[1], Min Lee[1], Yuchen Xu[1], Ratnesh Lal[1], Gert Cauwenberghs[1]

***Abstract*— In the wake of the COVID-19 pandemic, there has been a need for reliable diagnostic testing. However, state-of-the-art detection methods rely on laboratory tests and also vary in accuracy. We evaluate that the usage of a graphene field-effect-transistor (GFET) coupled with machine learning can be a promising alternate diagnostic testing method. We processed the current-voltage data gathered from the GFET sensors to assess information about the presence of COVID-19 in biosamples. We perform binary classification using the following machine learning algorithms: Linear Discriminant Analysis (LDA), Support Vector Machines (SVM) with the Radial Basis Function (RBF) kernel, and K-Nearest Neighbors (KNN) in conjunction with Principal Component Analysis (PCA). We find that LDA and SVM with RBF proved to be the most accurate in identifying positive and negative samples, with accuracies of 99% and 98.5%, respectively. Based on these results, there is promise to develop a bioelectronic diagnostic method for COVID-19 detection by combining GFET technology with machine learning.**

I. INTRODUCTION

Testing oneself for SARS-CoV-2 during the COVID-19 pandemic has been a crucial step toward promoting global health. The two most common state-of-the-art testing methods include laboratory reverse transcription polymerase chain reaction (RT-PCR) and rapid antigen testing [1]. However, one of the limitations of PCR testing is its reliance on centralized laboratories to get results [2]. Additionally, compared to the other methods, rapid antigen testing has a relatively high tendency to spark false negatives [3]. As such, there is a need to develop alternative methods of COVID-19 detection, such as through applications of electronics, artificial intelligence, and other indirect detection techniques.

One up-and-coming technology for COVID-19 diagnostic testing is the graphene field-effect-transistor (GFET), as mentioned in a previous paper [4]. A GFET sensor utilizes an electric field to detect changes in biomolecule concentration [5]. The GFET has three pins – the source, drain, and gate. By applying a range of gate voltages, the output drain current creates a current-voltage (I-V) curve. For viral detection, the GFET is functionalized with ssDNA (single-stranded DNA) aptamers that bind to a specific target protein on the virus of interest [6]. Through this, the viral analytes bind to the aptamers located on the GFET to cause a change in drain current. This shift in the drain current is known as the Dirac shift. Fig. 1 provides a depiction of the effect of binding a viral analyte onto the aptamer on the I-V curve.

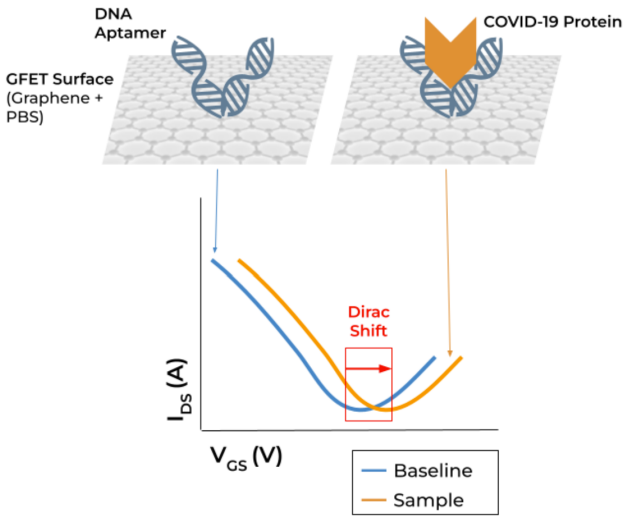

Fig. 1. Schematic diagram of the surface of a functionalized graphene field-effect-transistor (GFET) showing an aptamer with selective binding affinity to the analyte, in this case a COVID-19 protein. A binding of an analyte causes a Dirac shift in the I-V curve.

Despite advances in GFET development, there is limited research proving that a GFET-based system could function as an automatic viral detection system. In this paper, we build on the work done in [4] and propose that interfacing a GFET system with machine learning can be an effective diagnostic testing platform for COVID-19 detection.

II. METHODS

A. Preparation of GFET System

The GFET sensors were manufactured in an external facility, with the specifications detailed in [4]. The GFETs were functionalized with the aptamer for the SARS-CoV-2 nucleocapsid (N) protein. 10μL of phosphate-buffered saline (PBS) containing 1μM of the aptamer was added to the GFET chips.

The drain-source voltage (V_{DS}) was fixed at 100mV. The gate-source voltage (V_{GS}) was swept from -0.5 V to +1.5

[1]Darin Tsui, Francisco Downey, Shreenithi Navaneethan, Akshay Paul, Tyler Bodily, Min Lee, Yuchen Xu, Ratnesh Lal, and Gert Cauwenberghs are with the Shu Chien - Gene Lay Dept. of Bioengineering, University of California San Diego.
dtsui@ucsd.edu, fdowney@ucsd.edu, shnavane@ucsd.edu, a1paul@eng.ucsd.edu, tbodily@ucsd.edu, msl052@ucsd.edu, yux013@eng.ucsd.edu, rlal@ucsd.edu, gcauwenberghs@ucsd.edu

V, which we will refer to as a forward sweep, and then swept from +1.5 V to -0.5 V, which we will refer to as a backward sweep [4]. This forward/backward sweep sequence was carried out four times (4 forward and 4 backward sweeps total). The drain-to-source current (I_{DS}) was recorded to create the I-V characteristic curve from the V_{GS} voltage sweep. The I-V curve illustrates the Dirac point (global minimum of the I-V curve) of each sweep, which has been used extensively as an indicator of aptamer-target binding events. A visual depiction of the input pins for V_{DS} and V_{GS}, output pin for I_{DS}, and the holding well for the biosample is shown in Fig. 2.

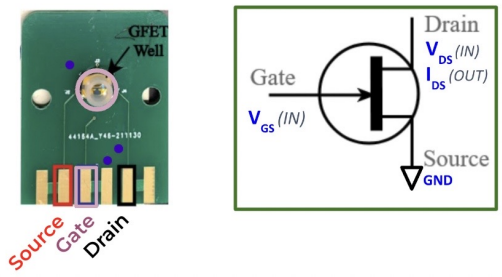

Fig. 2. Image and schematic diagram of the surface of a graphene field-effect-transistor (GFET) showing voltages input at the gate (V_{GS}) and drain (V_{DS}), and current output at the drain (I_{DS}).

The GFET chips were run through Fig. 3 to obtain their I-V curves. To collect data, a connection from the Keithley source measuring unit (SMU) to the GFET sensor was accomplished by ensuring metal contact with the three GFET sensor pins.

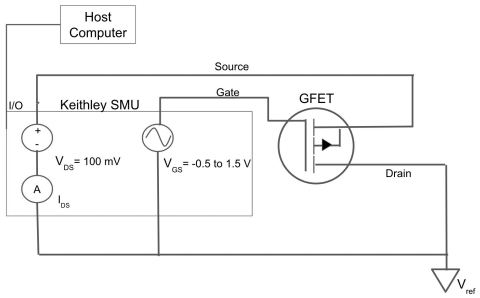

Fig. 3. Instrumentation diagram (above) of the GFET measurement depicts a computer-controlled dual-channel source meter (Keithley) driving the V_{GS} waveform while simultaneously recording the I_{DS} signal.

B. Data Collection

To explore machine learning methods for differentiating between viral and non-viral samples, we obtained the I-V curves for 19 test samples. 9 of the samples contained the Omicron strain of COVID-19, and will be referred to as the positive samples. The 10 negative samples contain no traces of COVID-19. The data collected for this machine learning analysis was taken in part from previous work done at the University of California San Diego [4].

Before adding the samples, 0.1X PBS was added to the GFETs and ran through the GFET interface shown in Fig. 3 to obtain their I-V curves. This initial curve generation will be defined as the baseline run. The saliva-virus samples were then added to the GFET, and after a few minutes of incubation for aptamer-target binding, the I-V curves were obtained. This will be defined as the sample run.

I-V curves were generated for all 19 samples to obtain their baseline and sample runs. 1000 I-V points were collected from each run on a GFET sensor. Here, each run was comprised of 8 voltage sweeps (4 forward sweeps and 4 backward sweeps, as mentioned in *Preparation of GFET System*).

The data being used was derived from each GFET sensor configured with either the Keithley SMU or the PIVOT, a handheld device that can run the GFET sensor and output the curves [4]. The data includes outputs from both baseline and sample runs for the given sensor. All the positive samples used in this study were run on GFET sensors that were functionalized with an aptamer for the Omicron variant of COVID-19.

C. Pre-processing and Feature Extraction

Upon obtaining the I-V curves, we separated them into forward and backward sweeps. For each sweep, we created three feature spaces to be used for the machine learning portion.

We refer to the first feature space as the Dirac Set, which involves identifying the I-V point corresponding to the Dirac point of each sweep. The Dirac Set is created by extracting the Dirac point from a single baseline sweep and a single sample sweep taken from the same chip and experimental test. Four dimensions constitute the Dirac Set: voltage corresponding to the baseline Dirac point, voltage corresponding to the sample Dirac point, current corresponding to the baseline Dirac point, and current corresponding to the sample Dirac point.

The second feature space, the Curve Estimation Set, also involves finding the Dirac point of the sweeps, as well as taking 4 evenly spaced I-V points between the Dirac point and each end of the curve (9 points total). We used these spaced-out points to create a 36-dimensional feature space (9 points multiplied by the same 4 dimensions mentioned in the previous feature space). Lastly, we create the All Points Set, which we take all the points from the I-V curve to create our feature space. These points create a 4*N dimensional feature space, where N is the total number of I-V points. Fig. 4 displays a visual overview of all feature sets.

D. Model Training and Testing

We trained and tested three different models using our feature sets to explore the possibility of classifying positive and negative samples based on GFET curves. The three models that were trained and tested in this paper include Linear Discriminant Analysis (LDA), Support Vector Machine with the Radial Basis Function (RBF) kernel, and K-Nearest Neighbors (KNN) with Principal Component Analysis (PCA). We tested these models using ten-fold cross-validation. We report accuracy, precision, and recall for all of the models.

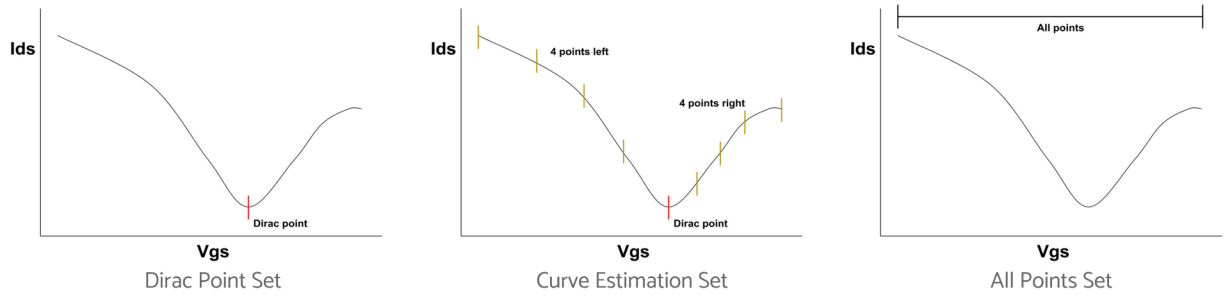

Fig. 4. Overview of the feature sets used.

III. Results

A. Visual Inspection of I-V Samples

Given that the machine learning results returned high accuracies, we looked to visualize our results. Fig. 5 illustrates the visual differences between negative and positive samples. We plotted the entire run of one of the negative and positive samples. It can be seen that the baseline and sample sweep in the negative case overlaps with each other. However, there appears to be a horizontal shifting of the sample sweep from the baseline sweep in the positive case. This change makes sense in the positive case since the addition of the COVID-19 biosample modulates the transfer of charges across the graphene.

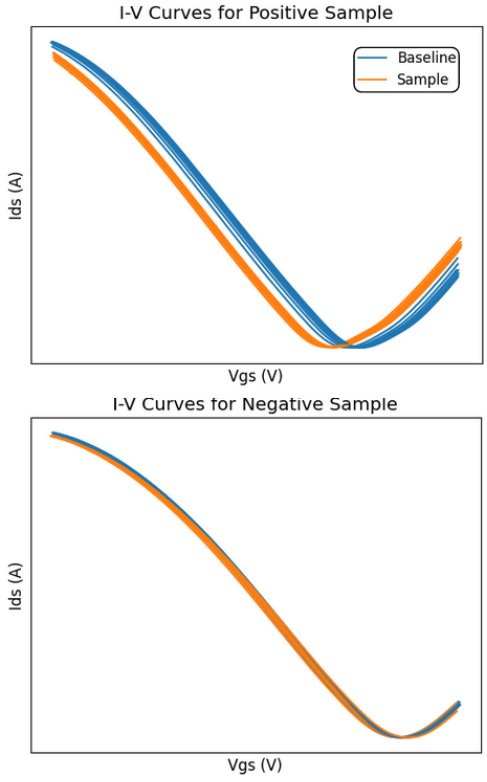

Fig. 5. I-V curves from a single run of a positive sample (above) and a negative control sample (below) applied to the GFET sensor.

The conventional approach to GFET curve classification entails evaluating the absolute difference in Dirac voltage between the baseline and sample curves, followed by establishing a linear decision boundary for positive and negative sample classification. Fig. 6 displays the manual decision boundary created that maximizes the testing accuracy. Using this method, we were able to get an accuracy of 68.4%.

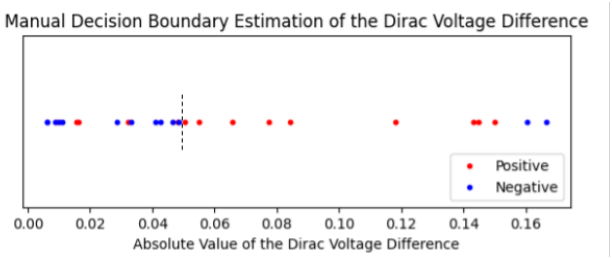

Fig. 6. Manual classification of the absolute value of the Dirac voltage differences between the baseline and sample runs.

Fig. 7 displays one testing fold of the class labels that LDA predicts for the Dirac Set and Curve Estimation Set, respectively. We plot only the Dirac points of the sample curve along their linear discriminant. Here, we are able to see a clear separation between positive and negative samples.

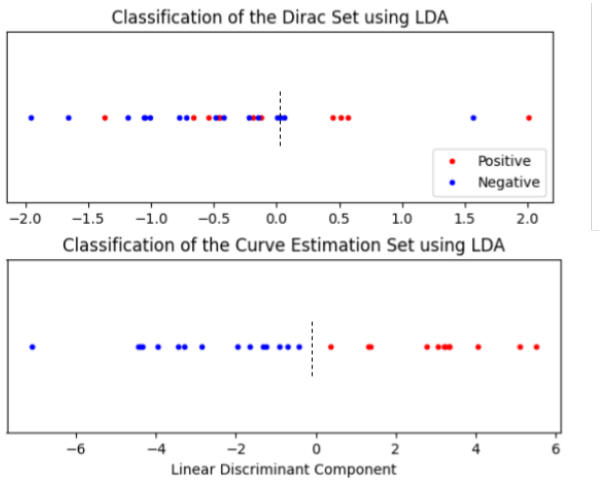

Fig. 7. Classifications of the Dirac and Curve Estimation Sets using LDA.

B. Performance of Machine Learning Models

Tables I, II, III report the accuracy, precision, and recall from the Dirac, Curve Estimation, and All Points Set.

TABLE I

CLASSIFICATION RESULTS FOR THE DIRAC FEATURE SET.

Classifiers	Accuracy	Precision	Recall
LDA	0.657	0.499	0.688
SVM and RBF	0.985	0.967	1.000
PCA + KNN	0.951	0.897	1.000

TABLE II

CLASSIFICATION RESULTS FOR THE CURVE ESTIMATION FEATURE SET.

Classifiers	Accuracy	Precision	Recall
LDA	0.962	0.935	0.986
SVM and RBF	0.928	0.848	1.000
PCA + KNN	0.934	0.892	0.967

TABLE III

CLASSIFICATION RESULTS FOR THE ALL POINTS FEATURE SET.

Classifiers	Accuracy	Precision	Recall
LDA	0.990	0.994	0.986
SVM and RBF	0.892	0.849	0.926
PCA + KNN	0.753	0.786	0.732

It can be seen in Table I that SVM with RBF recorded the highest accuracy using the Dirac Feature Set at 98.5%. In Table II, LDA recorded the highest accuracy using the Curve Estimation Feature Set at 96.2%. Finally, in Table III, LDA recorded the highest accuracy using the All Points Feature Set at 99%.

IV. DISCUSSION

A. Viral Sample Classification

When using LDA, accuracy, precision, and recall all significantly improved as a result of adding additional points to characterize the curves rather than just the Dirac points. This was most likely because LDA assumes that the given classes are linearly separable, and performance generally improves upon inputting additional data [7]. Additionally, SVM interfaced with RBF performed exceptionally well in the Dirac Set. This is most likely because by fitting a nonlinear decision boundary, we were able to increase the complexity of our model to accommodate the limited feature space [8].

Despite the limited dataset used, the high accuracy, precision, and recall scores achieved in all feature sets suggest that GFET sensors interfaced with machine learning could be a promising pipeline for effective COVID-19 diagnostic testing. With further optimization, it may be possible to develop a multi-class classification model that is able to detect distinct mutations in a virus using a single aptamer or detect entirely different viruses besides COVID-19.

B. Future Considerations

In addition to further studying the use of machine learning methods for more robust classification, optimizing the data collection process could result in improving the performance of the GFET. For example, as an alternative to maintaining a constant V_{DS}, one could vary V_{GS} while inputting an alternating V_{DS}. Furthermore, instead of using V_{DS} and V_{GS} as inputs, an alternating I_{DS} and V_{GS} could be utilized to obtain an output of V_{DS}. These variations could possibly reduce sensor drift, which ultimately would lead to better performance of the sensor. Optimizing GFET parameters could potentially improve classification accuracy on machine learning results.

V. CONCLUSION

In this study, we have shown that GFET sensors interfaced with machine learning have promising potential for effective COVID-19 detection. We performed binary classification on samples that were positive and negative for COVID-19 using current-voltage data generated from the GFETs on the following algorithms: LDA, SVM with the RBF kernel, and KNN with PCA. We find that using LDA as well as SVM with RBF achieved accuracies of 99% and 98.5%, respectively. Future work will be devoted to optimizing the GFET data collection process, as well as exploring multi-class classification of different viral mutations.

ACKNOWLEDGMENTS

The authors of this paper would like to thank members of the Integrated Systems Neuroengineering Lab and the Lab for Nano-bio-imaging and Devices in the Shu Chien - Gene Lay Department of Bioengineering, as well as the University of California San Diego Bioengineering Senior Design program's professor Dr. Bruce Wheeler and teaching assistant Anahid Foroughishafiei for all their support and guidance.

REFERENCES

[1] B. Giri, S. Pandey, R. Shrestha, K. Pokharel, F. S. Ligler, and B. B. Neupane, "Review of analytical performance of COVID-19 detection methods," Analytical and Bioanalytical Chemistry, Sep. 2020, doi: https://doi.org/10.1007/s00216-020-02889-x.

[2] A. Afzal, "Molecular diagnostic technologies for COVID-19: Limitations and challenges," Journal of Advanced Research, vol. 26, pp. 149–159, Aug. 2020, doi: https://doi.org/10.1016/j.jare.2020.08.002.

[3] G. Liu and J. F. Rusling, "COVID-19 Antibody Tests and Their Limitations," ACS Sensors, vol. 6, no. 3, pp. 593–612, Feb. 2021, doi: https://doi.org/10.1021/acssensors.0c02621.

[4] D. K. Ban et al., "Rapid self-test of unprocessed viruses of SARS-CoV-2 and its variants in saliva by portable wireless graphene biosensor," Proceedings of the National Academy of Sciences, vol. 119, no. 28, Jun. 2022, doi: https://doi.org/10.1073/pnas.2206521119.

[5] G. Seo et al., "Rapid Detection of COVID-19 Causative Virus (SARS-CoV-2) in Human Nasopharyngeal Swab Specimens Using Field-Effect Transistor-Based Biosensor," ACS Nano, vol. 14, no. 4, pp. 5135–5142, Apr. 2020, doi: https://doi.org/10.1021/acsnano.0c02823.

[6] J. Sengupta and C. M. Hussain, "Graphene-based field-effect transistor biosensors for the rapid detection and analysis of viruses: A perspective in view of COVID-19," Carbon Trends, p. 100011, Dec. 2020, doi: https://doi.org/10.1016/j.cartre.2020.100011.

[7] Balakrishnama, Suresh, and Aravind Ganapathiraju. "Linear discriminant analysis-a brief tutorial." Institute for Signal and Information Processing, Jan. 1998, pp. 1-8.

[8] C. Cortes and V. Vapnik, "Support-vector networks," Machine Learning, vol. 20, no. 3, pp. 273–297, Sep. 1995, doi: https://doi.org/10.1007/bf00994018.